J Electroceram (2012) 28:1–9
DOI 10.1007/s10832-011-9670-7

Magnetic properties of Ni-Zn ferrites prepared by microwave sintering method

M. Penchal Reddy · W. Madhuri · N. Ramamanohar Reddy · K. V. Siva Kumar · V. R. K. Murthy · R. Ramakrishna Reddy

Received: 28 November 2009 / Accepted: 22 November 2011 / Published online: 2 December 2011

Abstract The effect of zinc ion substitution for nickel on structural and magnetic properties of NiZn ferrites is reported. The spinel ferrite system $Ni_{1-x}Zn_xFe_2O_4$ with x= 0.2, 0.3, 0.4 and 0.5 was prepared by microwave sintering method. The uniaxially pressed samples were sintered at various temperatures such as 900°C, 1000°C and 1100°C for 30 min. X-ray diffraction patterns of the samples indicate the formation of single-phase cubic spinel structure. SEM micrographs show that grain size increases with increasing zinc content and sintering temperature. The elemental composition of these ferrites was analyzed by EDS. Lattice constant increases with increase in zinc content, obeying Vegard's law. The effect of composition and sintering temperature on initial permeability as the function of frequency and temperature was studied. The initial permeability of NiZn ferrite increases greatly with increasing Zn content and sintering temperature. The dependence of initial permeability with respect to temperature shows the decrease in the Curie point with increase in zinc content, is the normal behavior of ferrites. The relative loss factor $(\tan\delta/\mu_i)$ of the order of 10^{-2} to 10^{-5} in the frequency range from 100 Hz to 1 MHz indicates that the prepared ferrites have relatively high purity.

Keywords Ceramics · X-ray diffraction · Microstructure · Magnetic properties

M. P. Reddy (✉) · K. V. S. Kumar · R. R. Reddy
Department of Physics, Ceramic Composite Materials Laboratory,
Sri Krishnadevaraya University,
Anantapur 515 055, India
e-mail: penchu321@gmail.com

W. Madhuri
School of Advanced Sciences, VIT University,
Vellore 632014, India

N. R. Reddy
Department of Materials Science and Nanotechnology,
Yogi Vemana University,
Kadapa 516 227, India

V. R. K. Murthy
Microwave laboratory, Indian Institute of Science,
Chennai 600 036, India

1 Introduction

Ceramic ferrites are magnetic materials composed of selected oxides with iron oxides. The most common commercial soft magnetic materials are spinel ferrites, Ni-Zn and Mn-Zn ferrites having the general structure AB_2O_4. The Ni-Zn ferrite is preferred for low and higher frequency applications generally for power transformers, power inductors, micro wave devices, read and write heads for high speed digital tape, etc. because of their high resistivity, low losses, mechanical hardness, high Curie temperature and chemical stability [1–6]. The magnetic properties of ferrites are highly dependent on chemical composition, crystal structure, grain size and porosity. It is a well-known fact that the properties of ferrite materials are strongly influenced by the material's composition and microstructure. Due to their various technological applications, NiZn ferrites have attracted recently considerable research interest. The ferrites, in powder, pillets or in thin film forms, were prepared by the high-temperature solid state reaction method [7], coprecipitaion [8], sol–gel method [9], pulsed laser deposition [10], high-energy ball milling [11], hydrothermal technique [12], and flash combustion technique [13]. Several workers have successfully prepared Ni-Zn ferrites by the microwave sintering technique [14–18].

Use of microwave energy for synthesis and processing of materials is an exciting new field in material science with

enormous potential for synthesizing new materials and novel microstructures [19, 20]. The growing interest during the past decade is essentially due to the possibility of a reduction in manufacturing cost on account of energy savings, high energy efficiency, shorter processing times and improved product uniformity and yields [21].

The essential difference in the conventional and microwave sintering processes is in the heating mechanism. In conventional sintering, heat is generated by external heating elements and then it diffuses into the test sample via radiation, conduction and convection producing high temperature gradients and internal stresses [22]. In microwave sintering, the heat is generated internally within the test sample, by rapid oscillation of dipoles at microwave frequencies [23], instead of diffusion from external sources. As a result of this internal and volumetric heating, it is possible to sinter the materials rapidly and uniformly.

Many researchers have successfully synthesized Ni [24], Ni-Zn [17, 25] and Ni-Cu-Zn [14, 26–28] ferrites by employing the microwave sintering technique and studied their magnetic and electrical properties. In the present work, the authors aimed to study the effect of composition and sintering temperature on initial permeability as a function of frequency and temperature for $Ni_{1-x}Zn_xFe_2O_4$ (x=0.2, 0.3, 0.4 and 0.5) system prepared by microwave sintering technique.

2 Experimental

2.1 Preparation of $Ni_{1-x}Zn_xFe_2O_4$

The ferrite samples of composition $Ni_{1-x}Zn_xFe_2O_4$ (x= 0.2, 0.3, 0.4 and 0.5) were prepared employing the microwave sintering technique using analytical grade NiO, ZnO and Fe_2O_3. A stoichiometric solid-state high temperature reaction of metal oxides to form NiZn ferrites is as follows:

$$(1-x)\,\mathrm{NiO} + x\,\mathrm{ZnO} + \mathrm{Fe_2O_3} \rightarrow \mathrm{Ni_{1-x}Zn_xFe_2O_4} \qquad (1)$$

These constituent oxides were weighed, intimately mixed and the resulting powders were ball milled using a planetary ball mill (Restch PM 200, Germany) in agate bowls with agate balls in aqueous medium for 20 h. The slurry was dried and loosely pressed into cakes using a hydraulic press. These cakes were pre-sintered at a temperature of 800°C for 4 h in closed alumina crucibles. The pre-sintered cakes removed from the furnace were crushed and ball milled in an aqueous medium in agate bowls with agate balls for another 30 h to obtain fine particle size. These slurries after drying were sieved to obtain a uniform particle size. The green powder thus obtained was pressed in the form of toroids having dimensions 12 mm OD, 8 mm ID and 4 mm height and pellets having dimensions of thickness 2 mm and cross-sectional area 10 mm in diameter with a hydraulic press at a pressure of 200 MPa using 2% PVA solution as a binder with a suitable die.

2.2 Microwave sintering

The microwave furnace used in the present work is, a commercially available modified domestic (SHARP) microwave oven with a single magnetron operating at 2.45 GHz frequency, at an output power of 1.1 kW. The microwave furnace consists of a Eurotherm temperature controller, a Pt–Rh thermocouple assembly and a susceptor assembly. It is capable of operating up to 1400°C without any difficulty (Fig. 1).

2.2.1 Susceptor assembly

The susceptor assembly is an important unit of the microwave furnace. Tsay et al. [15] have used a porous Al_2O_3–SiO_2 crucible with SiC rods as susceptors which lead to uneven absorption of microwave energy, while others [17, 29] used SiC plates as susceptors. However, they have reported cracks in the samples due to rapid heating. Tsakaloudi et al. [18] used Y_2O_3 stabilized ZrO_2 refractory tiles on SiC plates as susceptors to avoid direct chemical interaction of SiC with ferrite samples beyond 1300°C. In this work the susceptor assembly was designed using a porous rectangular alumina block (Fig. 2(a)). The centre of this alumina block was scooped out to house an alumina crucible of 4 cm diameter and 4 cm height. An alumina lid with a hole at the centre to house the sensor was also provided to avoid zinc evaporation from the test samples. The microwave energy does not heat the alumina block directly because of its low dielectric loss. In order to overcome this difficulty, a 1 cm gap was provided in between the

Fig. 1 Microwave furnace

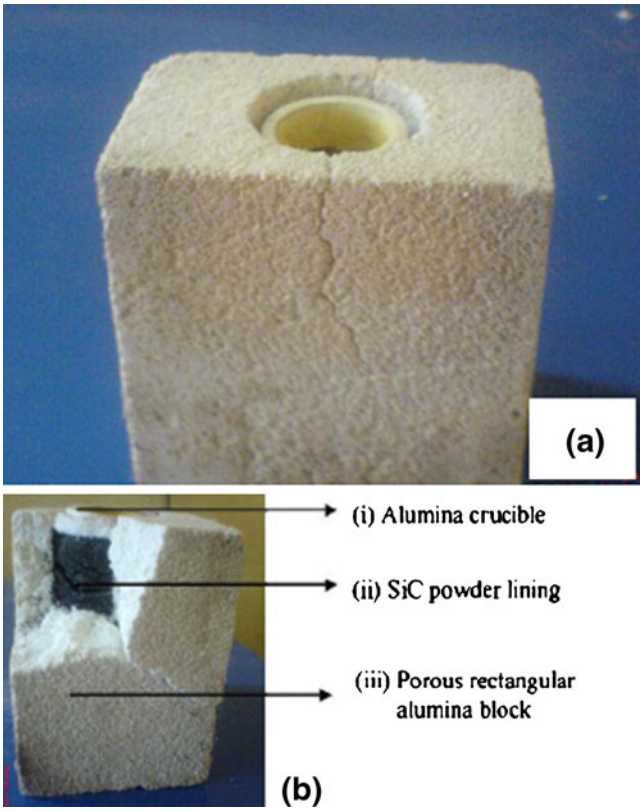

Fig. 2 (**a**) Susceptor, (**b**) susceptor showing SiC lining: (i) alumina crucible, (ii) SiC powder packing and (iii) porous rectangular alumina block

alumina block and the alumina crucible. This space was packed very tightly with fine SiC powder (Fig. 2(b)). A ceramic fiber based casketing around this alumina block permits the transport and concentration of microwave radiations but provides a negligible thermal load on insulation. This type of fabrication of s susceptor assembly works well without any thermal gradients during microwave heating.

2.2.2 Thermocouple assembly

The temperature was measured using the Pt–Rh thermocouple assembly. It consisted of an inner fused silica tube holding the Pt–Rh thermocouple couple. One end of the fused silica tube was capped with a thin platinum foil and the foil was earthed. Enough care was taken to see that the Pt foil does not touch the thermocouple bead. This entire assembly was housed in a crystallized alumina sheath. This thermocouple was calibrated using an optical pyrometer (Leeds and Northrup). This sensor was housed very close to the test sample taking proper care not to bring it into contact with the sample.

The green pressed samples were first heated to 120°C in a separate oven and kept for 2 h for moisture removal prior to loading of the samples into the microwave furnace. The compacted samples were sintered at three different temperatures of 900, 1000 and 1100°C, for 30 min. The microwave furnace was operated with a total run time of 35–40 min and an average soaking time of 30 min at 900, 1000 and 1100°C. No attempt was made to include the binder burring step during the sintering schedule. The microwave sintered samples were found to be without any visible cracks.

2.3 Experimental techniques used for characterization and initial permeability measurement

The physical density of the specimens has been determined by Archimedes principle. The X-ray diffraction (XRD) patterns of ferrites studied in this work were recorded using an x-ray diffraction system (PM 1730, Germany) using Cu K_α radiation. The microstructure of the sintered samples was examined by scanning electron microscope (SEM) using CRL-ZESIS-EVO-MAI5 model. The compositions of the sintered samples were confirmed using an energy-dispersive x-ray spectrometry (EDS) facility attached to the scanning electron microscope. Energy-dispersive X-ray spectroscopy (EDX) was used to determine the final composition of the samples. The initial permeability (μ_i) of these ferrite toroids were evaluated using the standard formulae from the inductance measurements carried out using a computer controlled impedance analyzer (Hioki Model 3532–50 LCR HiTester, Japan) in the frequency range from 100 Hz to 1 MHz (at constant room temperature) and temperature from room temperature to Curie point (at constant frequency, 1 kHz and 10 kHz). These measurements were carried out in the temperature ranging from 30 to 550°C. The permeability was calculated by using the relation [30]:

$$L = 0.0046N^2\mu_i h\log_{10}\left(\frac{D_0}{D_i}\right) \quad (2)$$

Where L is the inductance in μH, h is the height of the toroid, D_0 and D_i are the outer and inner diameters and N is the number of turns (30–35 in this case) wound on the toroid.

3 Results and discussion

3.1 Phase identification

The X-ray diffracrograms of all the samples are presented in Fig. 3. The presence of planes (2 2 0), (3 1 1), (2 2 2), (4 0 0), (4 2 2), (5 1 1), (4 4 0), (6 2 0), (5 3 3), (6 2 2) and (4 4 4) in the diffractograms confirms the formation of cubic spinel structure.

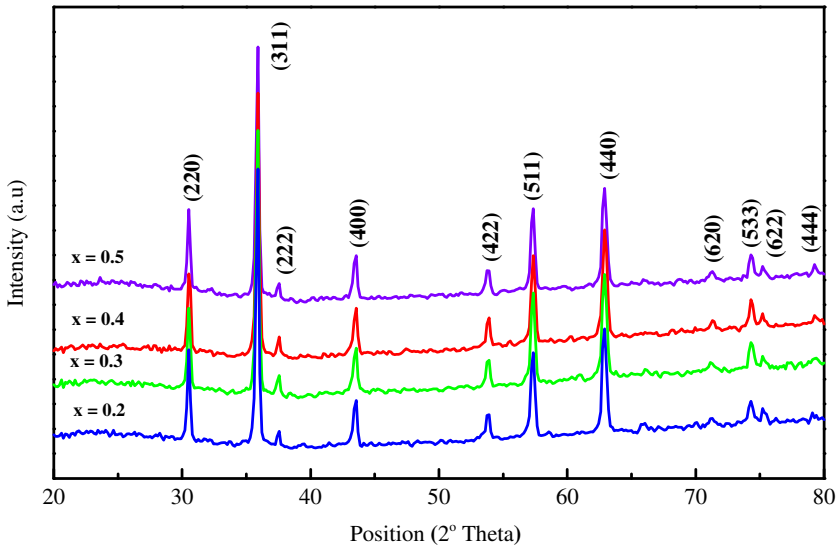

Fig. 3 XRD patterns of $Ni_{1-x}Zn_xFe_2O_4$ (x=0.2, 0.3, 0.4 and 0.5) prepared by microwave sintering technique

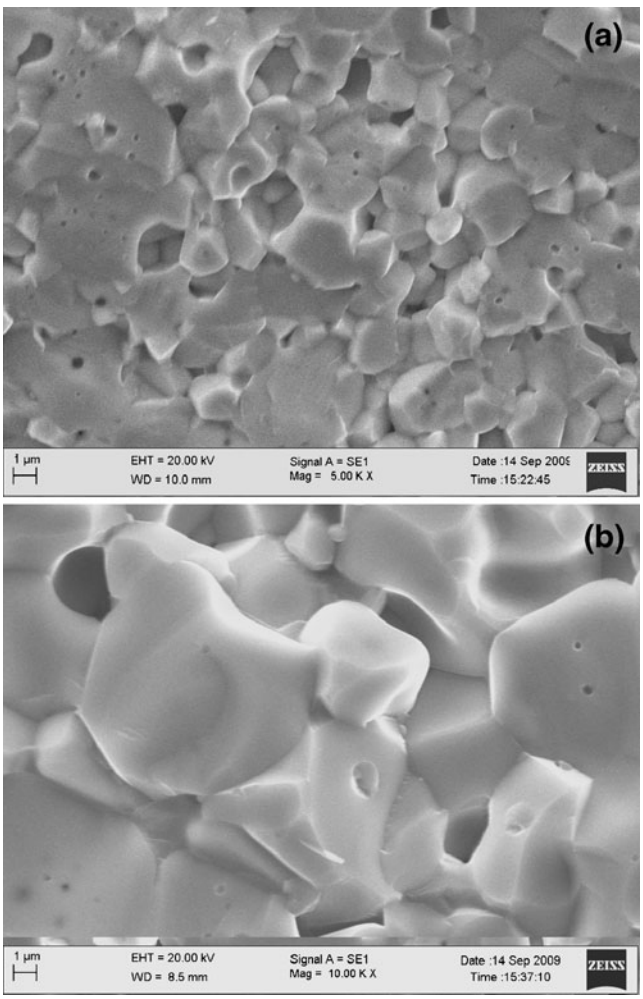

Fig. 4 SEM micrographs of fracture surfaces of (**a**) $Ni_{0.8}Zn_{0.2}Fe_2O_4$ and (**b**) $Ni_{0.5}Zn_{0.5}Fe_2O_4$ ferrites prepared by microwave sintering method and sintered at 1000°C

3.2 Microstructures of $Ni_{1-x}Zn_xFe_2O_4$

Figure 4 represents SEM micrographs of the samples. The SEM micrographs of the sintered samples were recorded to understand the microstructure of the Ni-Zn ferrites. The average grain size was determined using the relation [31]:

$$G_a = \frac{1.5L}{MN} \tag{3}$$

Where L is the total test line length; M is the magnification; N is the total number of intercepts.

The average grain size is observed to be 1.6, 10.4 µm for x=0.2, 0.5 respectively. From Table 1, it is observed that, the average grain size lies in the range from 1.8 to 11.3 µm. It is revealed that the grain size increases with increase in Zn content and sintering temperature. Similar results are reported by R.V. Mangalaraja et.al. [13]. This is due to fact

Table 1 Lattice constant, Sintering temperature, Density, Porosity, Curie transition temperature, Average grain size and Initial permeability data of $Ni_{1-x}Zn_xFe_2O_4$ system

x	a (Å)	T_s (°C)	ρ (gm/cm^3)	P (%)	T_c (°C)	G_a (µm)	μ_i (10 kHz)
0.2	8.332	900	4.65	28.2	470	1.2	89
		1000	4.79	24.6		1.9	159
		1100	5.94	21.4		2.4	296
0.3	8.335	900	4.82	26.3	410	2.1	281
		1000	4.99	22.4		3.4	374
		1100	5.08	19.1		4.3	518
0.4	8.337	900	5.04	23.4	340	3.8	435
		1000	5.13	21.2		5.7	612
		1100	5.24	18.5		7.9	799
0.5	8.339	900	5.22	21.5	260	8.5	952
		1000	5.36	17.8		10.4	1197
		1100	5.47	15.3		11.3	1393

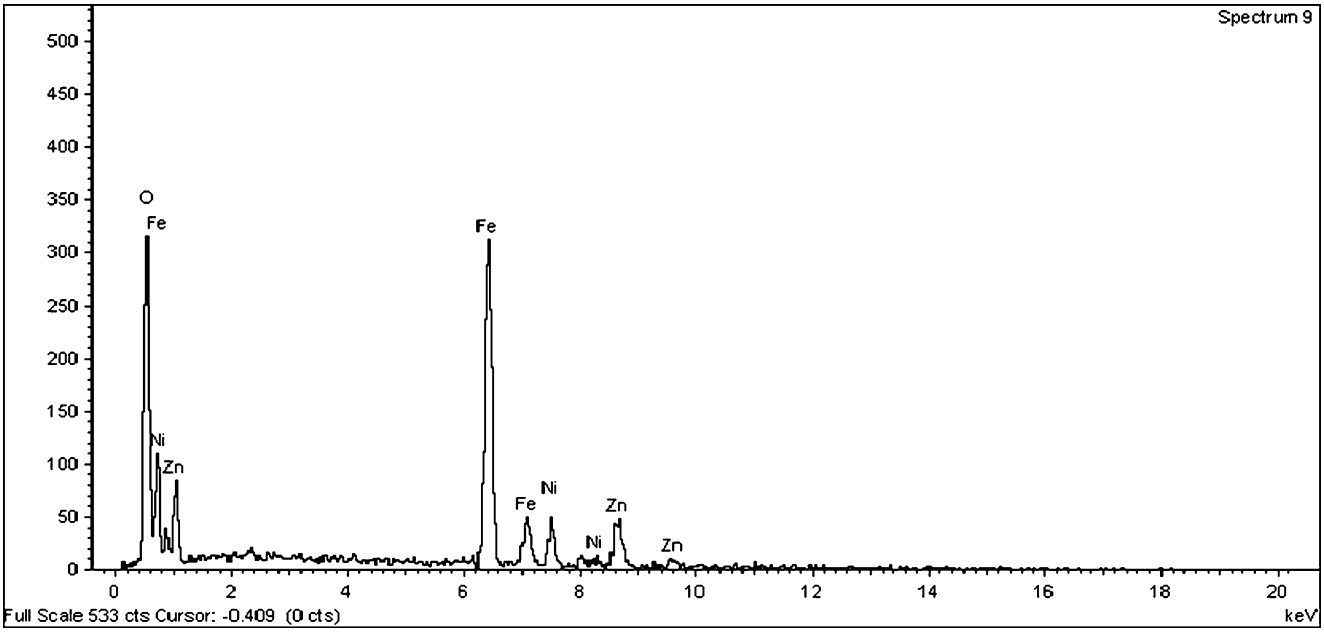

Fig. 5 EDS spectrum of $Ni_{0.5}Zn_{0.5}Fe_2O_4$ ferrites prepared by microwave sintering method and sintered at 1000°C

that the higher zinc content enhances sintering and it leads to higher grain growth [32]. It is also observed that grain size of the samples under investigation is bigger than that prepared by flash combustion technique [13] and oxalate precipitation method [33].

In order to confirm the chemical composition, EDS analysis was carried and is shown in Fig. 5. This compositional analysis method could accurately measure the Ni and Zn content, but was unable to give accurate results for O content [34].

3.3 Lattice parameter, bulk density and porosity of the $Ni_{1-x}Zn_xFe_2O_4$

The variation of lattice parameter 'a' as a function of Zn content (x) is depicted in Fig. 6. It is noticed that the lattice parameter increases with increase in zinc content, obeying Vegard's law. This variation can be explained on the basis of an ionic size difference of the component ions. The Zn^{2+} ions have a larger ionic radius (0.72 Å) than the Ni^{2+} (0.69 Å). The Zn^{2+} ions successively replace the Ni^{2+} ions in B-site. The unit cell expands to accumulate the larger ions. Thus addition of Zn^{2+} at the expense of Ni^{2+} in the ferrite is explained to increase the lattice parameter.

The lattice parameter, density, porosity and average grain size for different samples sintered at different temperatures are presented in Table 1. It is observed that the bulk density increases with increasing zinc content and sintering temperature. The small amount of zinc evaporation at higher temperature does not affect the sintered density of ferrites. It is also observed that the density of ferrite under investigation is higher than reported values of ferrite prepared by oxalate precipitation, ceramic and flash combustion method [33, 35, 36]. This suggests that microwave sintering favors higher densification and more compaction. On the other hand, porosity decreases with increasing sintering temperatures. Similar results are reported by R.V. Mangalaraja et.al [13]. Porosity values of various samples are presented in Table 1. It is known that the porosity of the ceramic samples results from two sources, intragranular porosity and intergranular porosity. Thus, the total porosity could be written as $P=P_{intra}+P_{inter}$. The intergranular porosity mostly depends on the grain size. At higher sintering temperatures grains are formed uniformly and voids are reduced, as a result density increases.

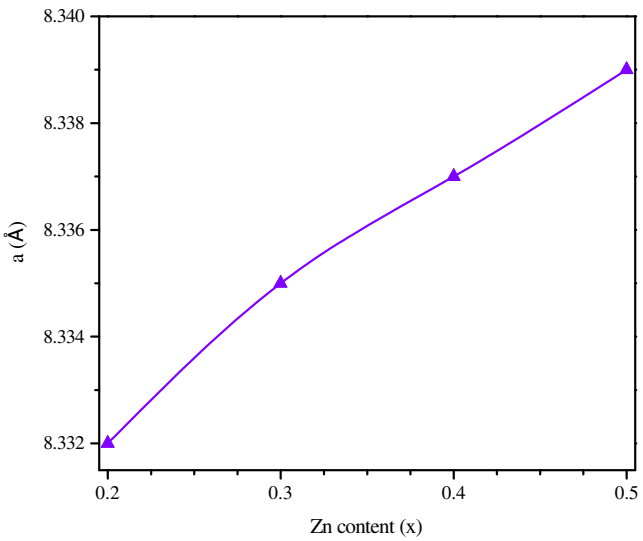

Fig. 6 Variation of lattice constant 'a' with Zn content (x) in $Ni_{1-x}Zn_xFe_2O_4$ ferrites

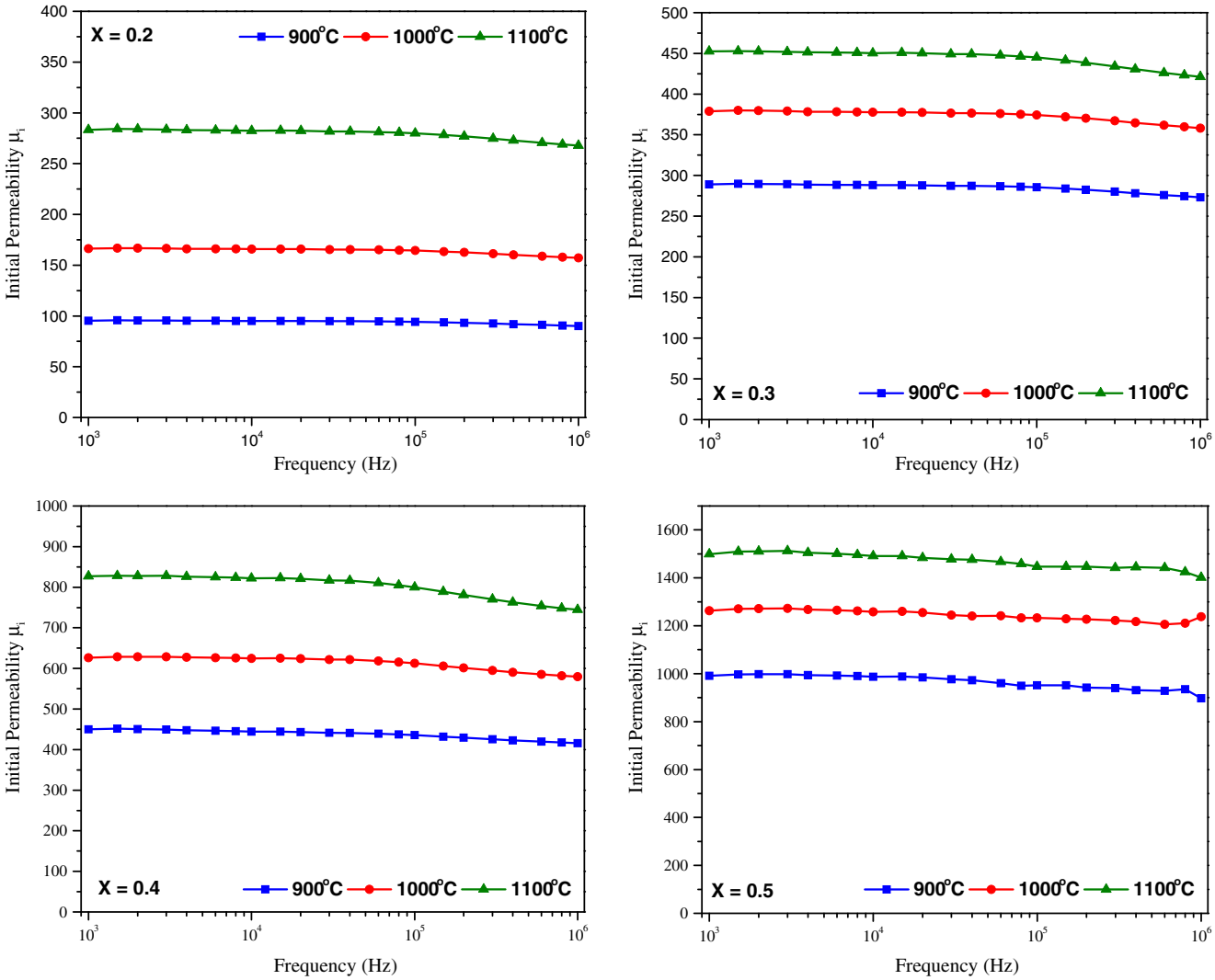

Fig. 7 Frequency dependence of Initial permeability (μ_i) for $Ni_{1-x}Zn_xFe_2O_4$ ferrites

3.4 Frequency dependence of initial permeability of $Ni_{1-x}Zn_xFe_2O_4$

The initial permeability is an important magnetic property to study the quality of soft ferrites. Figure 7 Shows the real part of initial permeability (μ_i) as a function of frequency in the range 100 Hz to 1 MHz for $Ni_{1-x}Zn_xFe_2O_4$ (x=0.2, 0.3, 0.4 and 0.5) sample prepared by microwave sintering method and sintered at three various temperatures of 900, 1000 and 1100°C for a period of 30 min. It is observed that magnetic initial permeability (μ_i) increases with sintering temperature. This is because pores and voids are reduced with increasing sintering temperature. The permeability of polycrystalline ferrite is related to two different magnetizing mechanisms: spin rotation and domain wall motion [37–40], which can be described as,

$$\mu_i = 1 + \chi_w + \chi_{spin}$$

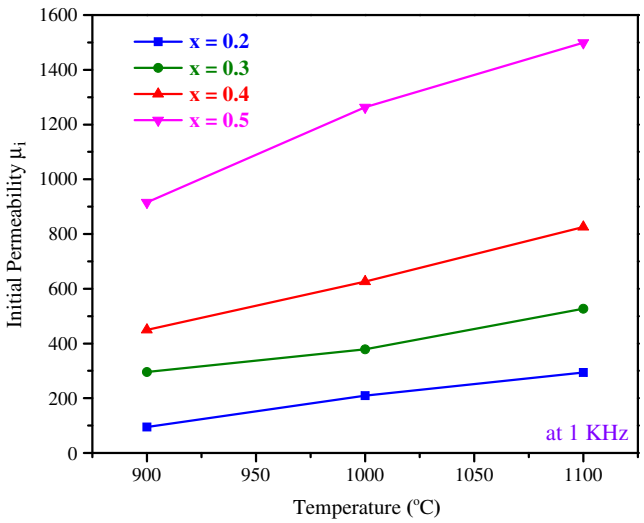

Fig. 8 Variation of initial permeability with sintering temperature for $Ni_{1-x}Zn_xFe_2O_4$ ferrites

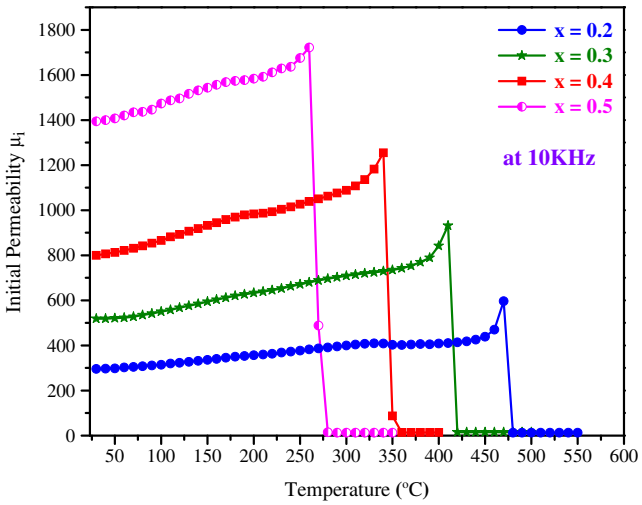

Fig. 9 Variation of initial permeability as a function of temperature for $Ni_{1-x}Zn_xFe_2O_4$ ferrites system sintered at 1100°C for 30 min

Where χ_w is the domain wall susceptibility, χ_{spin} spin is intrinsic rotational susceptibility. The χ_w and χ_{spin} spin may be written as

$$\chi_w = \frac{3\pi M_s^2 D}{4\gamma} \text{ and } \chi_{spin} = \frac{2\pi M_s^2}{K_u}$$

Where *M*s the saturation magnetization, *K*u the total anisotropy, *D* the average grain diameter, and γ the domain wall energy. Our microstructure study shows that the average grain diameter increases with increasing sintering temperature (Table 1). Therefore, an increase of (μ_i) with increasing sintering temperature is expected. The increase in the value of initial permeability (μ_i) with the sintering temperature which is shown in Fig. 8, causes the grain growth observed at higher temperature. It is also observed that the increase in zinc content increases the grain size [41] and density [28], and decreases the anisotropy [42], which results in an increase in the value of initial permeability. It is well known that the initial permeability characteristics depend not only on chemical composition but also on the microstructure of the sintered body. Desired magnetic properties of ferrite can be achieved by the control of microstructures [43].

3.5 Temperature dependence of initial permeability of $Ni_{1-x}Zn_xFe_2O_4$

The magnetic initial permeability as the function of temperature from room temperature to Curie temperature was also studied. The initial permeability (μ_i) as a function of temperatures for $Ni_{1-x}Zn_xFe_2O_4$ (x=0.2, 0.3, 0.4 and 0.5) compositions are shown in Fig. 9. The initial permeability (μ_i) was measured at a constant frequency (10 KHz) of a sinusoidal wave. It can be noted from figure that as the temperature increases the initial permeability (μ_i) remains constant up to a certain temperature and increases to a peak value and then abruptly falls to a minimum value. The temperature at which this abrupt fall takes place is the magnetic Curie transition temperature T_c. At this temperature the specimens transform from the ferrimagnetic phase to the paramagnetic phase. It is observed that the initial permeability increases with zinc content. The effect of zinc content on permeability/temperature (μ/θ) relation shows that as the amount of zinc content increases, there is a fall in Curie point and an increase in permeability. Also, it is clear that the Curie transition temperature decreases with increasing zinc ion content and is in agreement with the literature values [13, 42, 44]. This is

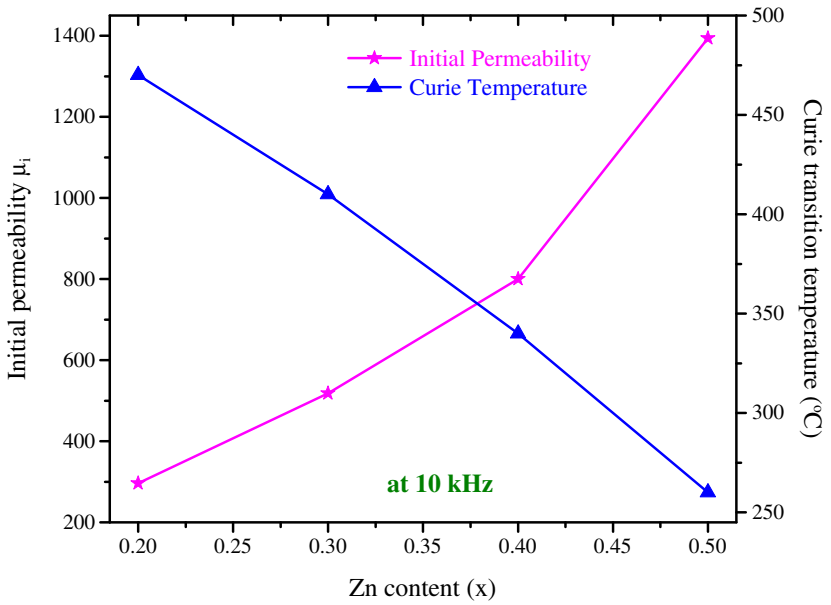

Fig. 10 Variation of initial permeability and Curie temperature for $Ni_{1-x}Zn_xFe_2O_4$ ferrites sintered at 1100°C

natural because zinc is a non-magnetic material, and therefore the progressive replacement of Ni ions with Zn ions lowers the Curie transition temperature. Due to the decrease in the magnetic ions at tetrahedral site decrease the interaction between tetrahedral and octahedral, thereby decreasing the Curie transition temperature.

3.6 Compositional dependence of initial permeability and Curie transition temperature

The substitution of Zn has a major effect on initial permeability (μ_i); with an increase in x from 0.2 to 0.5, the permeability increases from about 290 to 1390. On the other hand, the Curie temperature is decreased from 470 to 260. The effect of composition (x) on initial permeability and Curie transition temperature is summarized in Fig. 10. The initial permeability and Curie transition temperature show an inverse trend with each other. It is also observed that the magnetic initial permeability of ferrite prepared under investigation is higher than reported of magnetic initial permeability of ferrite prepared by ceramic [45] and flash combustion method [13].

Furthermore, the relative loss factor (tan δ/μ_i) was greatly reduced from 10^{-4} to10^{-5} at 100 kHz by using microwave sintering technique instead of the flash combustion technique. The relative loss factor is observed with increase in the zinc content. The sample with low zinc content exhibits lower loss values is due to insignificant zinc loss. The low loss value obtained in the present work indicates that the samples are relatively high purity. Ferrites with low relative loss factor values can be used as inductor and transformer materials in high frequency applications.

4 Conclusions

Microwave sintering is a very promising technique for the preparation of single phase Ni-Zn ferrites with low sintering temperature and smaller duration as compared to ceramic and flash combustion method. X-ray diffraction patterns confirm the formation of cubic spinel structure. The average grain size is found to increase with increase in zinc content, sintering temperature and it is attributed to the larger ionic size of Zn. The lattice parameter 'a' is found to increase with increasing zinc content. High density is obtained for ferrites prepared in microwave heating than in normal heating. The relative loss factor of the order of 10^{-2} to 10^{-5} obtained in the operating frequency indicates that the ferrites are relatively high purity. The zinc content in the Ni-Zn ferrite is an important factor for not only enhancing the densification of the ferrite but also for improving the magnetic properties of ferrites. The initial permeability increases with Zn content and sintering temperature. The increase in permeability can be attributed to the presence of Zn ions activating the sintering process in ferrites and leading to increase in density and grain size. Thus, it may be said that Zn substitution increases the densification at lower sintering temperature and activates the grain growth of the Ni-Zn ferrites. As a consequence, ZnO improves the magnetic initial permeability of these ferrites.

Acknowledgement The authors are thankful to the authorities of Sri Krishnadevaraya University, Anantapur for providing the facilities. This work was supported by the financial assistance provided by the Defence Research and Development Organization (DRDO), New Delhi, India. The authors wish to thank the Editor of the journal and the Anonymous Reviewers for their constructive and useful comments which improve the scientific content of the original paper.

References

1. H. Igarash, K. Okazaki, J. Am. Ceram. Soc. **60**, 51 (1977)
2. K. Kulikowski, J. Magn. Magn. Mater. **41**, 56 (1984)
3. P. Ravindranathan, K.C. Patil, J. Mater. Sci. **22**, 3261 (1987)
4. T. Abraham, Am. Ceram. Soc. Bull. **73**, 62 (1994)
5. P.I. Slick, in *Ferromagnetic Materials, vol. 2*, ed. by E.P. Wohlforth (North-Holland, Amsterdam, 1980), p. 196
6. B.V. Bhise, M.B. Dongare, S.A. Patil, S.R. Sawant, J. Mater. Sci. Lett. **10**, 922 (1991)
7. M. Arshed, M. Siddique, M. Anwar-ul-Islam, N.M. Butt, T. Abbas, M. Ahmed, Solid State Commun. **93**, 599 (1995)
8. A.S. Albuquerque, J.S. Ardisson, W.A.A. Macedo, J. Appl. Phys. **87**, 4352 (2000)
9. A. Chatterji, D. Das, S.K. Pradhan, D. Chakravorty, J. Mgn. Magn. Mater. **127**, 214 (1993)
10. F.W. Oliver, D. Seifu, E. Hoffman, D.B. Chisey, J.S. Horwitz, P.C. Dorsey, Appl. Phys. Lett. **75**, 2993 (1995)
11. C.N. Chinnasamy, A. Narayanasamy, N. Ponpandian, K. Chatopadhyay, H. Guerault, J.M. Greneeche, J. Phys. Condens. Mater. **12**, 7795 (2000)
12. C. Upadhyay, D. Mishra, H.C. Verma, S. Anand, R. Roy, Mater. Sci. Eng. B **98**, 188 (2003)
13. R.V. Mangalaraja, S. Thomas Lee, S. Ananthakumar, P. Manohar, C.P. Camurri, Mater. Sci. Eng., A **476**, 234 (2008)
14. C.Y. Tsay, K.S. Liu, T.F. Lin, I.N. Lin, J. Magn. Magn. Mater. **209**, 189 (2000)
15. C.Y. Tsay, K.S. Liu, I.N. Lin, J. Euro. Ceram. Soc. **21**, 1937 (2001)
16. Y.P. Fu, K.Y. Pan, C.W. Liu, Mater. Lett. **57**, 291 (2002)
17. P. Yadoji, R. Peelamedu, D. Agarwal, R. Roy, Mater. Sci. Eng. B **98**, 269 (2003)
18. V. Tsakaloudi, E. Papazoglou, V.T. Zaspalis, Mater. Sci. Eng. B **106**, 289 (2004)
19. B. Vaidhyanathan, A.P. Singh, D.K. Agarwal, T.R. Shrout, R. Roy, J. Am. Ceram. Soc. **84**, 1197 (2001)
20. W.H. Sutton, Ceram. Bull. **68**, 376 (1989)
21. V.K. Sankaranarayan, C. Sree Kumar, Curr. Appl. Phys. **3**, 205 (2003)
22. A.C.F.M. Costa, E. Tortella, M.R, Morelli, R.H.G.A. Kiminami. J. Magn. Magn. Mater. **256**, 174 (2003)
23. A.R. Phani, S. Santucci, J. Non-Cryst. Solids **352**, 4093 (2006)
24. V.K. Sankaranarayan, C. Sree Kumar, Cur. Appl. Phys. **3**, 205 (2003)
25. Y.J. Yang, C.I. Sheu, S.Y. Cheng, H.Y. Chang, J. Magn. Magn. Mater. **284**, 220 (2004)

26. H. Saita, Y. Fang, A. Nakano, D. Agrwal, M.T. Langan, T.R. Shrout, C.A. Randall, Jpn. J. Appl. Phys. **41**, 86 (2002)
27. M. Yan, J. Hu, J. Magn. Magn. Mater. **305**, 171 (2006)
28. M. Penchal Reddy, W. Madhuri, M. Venkata Ramana, N. Ramamanohar Reddy, K. Siva Kumar, V.R.K. Murthy, K.V. Siva Kumar, R. Ramakrishna Reddy, J. Magn. Magn. Mater. **322**, 2819 (2010)
29. T. Krishnaveni, S.R. Murthy, F. Gao, Q. Lu, S. Komarneni, J. Mater. Sci. **41**, 1471 (2006)
30. D. Bhosale, D.N. Choudhari, S.R. Sawant, R.D. Kale, P.P. Bakare, IEEE Trans. Magn. **34**, 535 (1998)
31. J.C. Wurst, J.A. Neslson, J. Am. Ceram. Soc. **55**, 109 (1972)
32. J. Smit, H.P.J. Wijn, *Ferrites* (Phililps Technical Library, Eindhovan, 1959), p. 221
33. T.J. Shinde, A.B. Gadkari, P.N. Vasambekar, Mater. Chem. Phys. **111**, 87 (2008)
34. J.A. Paulsen, C.C.H. Lo, J.E. Snyder, A.P. Ring, L.L. Jones, D.C. Jiles, IEEE Trans. Magn. **39**, 3316 (2003)
35. R.V. Mangalraja, S. Ananthakumar, P. Manohar, F.D. Gnanam, Matt. Lett. **57**, 1151 (2003)
36. R.V. Mangalraja, S. Ananthakumar, P. Manohar, F.D. Gnanam, M. Awano, Matt. Lett. **58**, 1593 (2004)
37. H. Jun, Y. Mi, J. Zhejiang, Univ. Sci. **6B**(6), 580 (2005)
38. T. Tsutaoka, M. Ueshima, T. Tokunaga, T. Nakamura, K. Hatakeyama, J. Appl. Phys. **78**(6), 3983 (1995)
39. A.K.M. Akther Hossain, K. Khirul Kabir, M. Seki, T. Kawai, H. Tabata, J. Phys. Chem. Solids. **68**, 1933 (2007)
40. A.K.M. Akther Hossain, H. Tabata, T. Kawai, J. Magn. Magn. Mater. **320**, 1157 (2008)
41. A. Beer, J. Schwarz, IEEE Trans. Magn. **2**(3), 470 (1996)
42. A. Verma, T.C. Goel, R.G. Mendiratta, R.G. Gupta, J. Magn. Magn. Mater. **210**, 274 (2000)
43. S.I. Pyun, J.T. Baek, Am. Ceram. Soc. Bull. **64**(4), 602 (1985)
44. E.C. Snelling, *Soft ferrites: properties and applications* (Butterworths, London, 1998)
45. J. Bera, P.K. Roy, Physica B **363**, 128 (2005)